Proc. Indian Acad. Sci. (*Chem. Sci.*), Vol. 113, No. 1, February 2001, pp 55–62

Small-angle neutron scattering study of sodium cholate and sodium deoxycholate interacting micelles in aqueous medium

J SANTHANALAKSHMI*[1], G SHANTHA LAKSHMI[1], V K ASWAL[2] and P S GOYAL[2]
[1]Department of Physical Chemistry, University of Madras, Guindy Campus, Chennai 600 025, India
[2]Condensed Matter Physics Division, Bhabha Atomic Research Division, Trombay, Mumbai 400 085, India
e-mail: jaysune@eth.net

MS received 21 July 2000; revised 23 November 2000

Abstract. Small angle neutron scattering (SANS) measurements of D_2O solutions (0·1 M) of sodium cholate (NaC) and sodium deoxycholate (NaDC) were carried out at T = 298 K. Under compositions very much above the critical micelle concentration (CMC), the bile salt micelle size growths were monitored by adopting Hayter–Penfold type analysis of the scattering data. NaC and NaDC solutions show presence of correlation peaks at Q = 0·12 and 0·1 Å^{-1} respectively. Monodisperse ellipsoids of the micelles produce best fits. For NaC and NaDC systems, aggregation number (9·0, 16·0), fraction of the free counterions per micelle (0·79, 0·62), semi-minor (8·0 Å) and semi-major axes (18·4, 31·7 Å) values for the micelles were deduced. Extent of micellar growth was studied using ESR correlation time measurements on a suitable probe incorporating NaC and NaDC micelles. The growth parameter (axial ratio) values were found to be 2·3 and 4·0 for NaC and NaDC systems respectively. The values agree with those of SANS.

Keywords. Biosurfactants; sodium deoxycholate micelles; bile salt micelles; SANS study; ESR correlation times.

1. Introduction

The role of bile salts (sodium cholate, NaC; sodium deoxycholate, NaDC) as physiological surfactants is based on their micelle-forming properties [1–3]. These represent the class of potential biosurfactants which play active roles as cholesterol and lipid solubilizers, emulsifiers and dispersion agents in cosmetics, medicines and chemicals [4–6]. Micellar properties of NaC and NaDC at nearly their respective critical micelle concentration (CMC) values have been reported in the literature based on different experimental techniques [7–10]. Also, NaC, NaDC and other bile salts exhibit concentration-dependent microstructures [11]. The vital bioactivities of bile salts are found at concentrations very much above CMC and are due to their micellar properties. Near CMC values, primary micelles with low aggregation numbers are detected, which at higher concentrations produce secondary or rod-like super-grown micelles [12,13]. In the NaC system, the CMC value for the primary micellization occurs around 0·013–0·018 M

*For correspondence

corresponding to the primary aggregates consisting of dimer units. At higher concentrations of NaC, around 0·05 M, secondary micellization is detected corresponding to enlarged dimensions of primary micelles [14,15]. Similarly for the NaDC system, around 0·01 M and 0·05 M primary and secondary micellizations are detected in presence of *p*H buffers. With further increase in the concentration of bile salts, a third micellization may set in, which may be super-grown secondary micelles with extended dimensions in size. In all, bile salt aggregation behaviour is strongly concentration-dependent and units of dimer are stacked through successive hydrophobic and H-bonds. Based on the experimental technique being adopted, accuracy in the detection of various stages of stepwise aggregation may be rendered possible. Surface tension studies on bile salt system under *p*H control prove to be of such kind. In such cases, exact estimations of the aggregation number, interaction potentials of micelles and the nature of the extended size growths in micelles are still ambiguous. Earlier reports on SANS of bile salts consist of radii and rod axis lengths, with *p*H and ionic strength effects [16–19].

The present work is devoted to adopting small angle neutron scattering (SANS) which is a powerful tool to investigate self-association patterns, for the study of secondary micelles of NaC and NaDC at 0·1 M concentrations in the absence of any additives. Scattering patterns are subjected to Hayter–Penfold analysis and using correlation peak positions, determination of many physicochemical parameters of the micelles such as the equivalent spherical radius [$R = (a^2b)^{1/3}$], semi-minor and semi-major axes (a, b), number density of micelles (N_m), surfactant aggregation number (N_{BS}), fraction of the free counterions per micelle (a_{BS}), micelle concentration [mic], Debye screening length (k^{-1}) and the mean intermicellar interaction potentials ($U(r)/U(T)$) from SANS are carried out for NaC and NaDC micelles at 298 K. In aqueous systems, the hydrodynamic equivalent spherical radii of the ionic secondary micelles vary sensitively with environmental conditions like *p*H, salt, temperature etc., just as they do for primary micelles [20,21]. Hence evaluation of microstructures of secondary micelles is essential. The evaluation of R_h of the bile salt micelles under compositions very much above CMC may be carried out using an ESR spin label technique [22]. In the present work, an anisotropy sensitive spin label such as 3-(2,2′-dimethyl-N-oxyl-oxazolidinyl)-5α-cholestane (CSL) (1×10^{-4} M) incorporated NaC and NaDC (0·1 M) micelle solutions are subjected to ESR measurements [23,24]. The analysis of the spectral line shapes and line widths can be performed in terms of rotational correlation time (t_R), which when applied with Stokes–Einstein equation, the effective hydrodynamic radius value of the micelle may be determined. Also the semi-major and semi-minor axes values of the ellipsoidal micelles are computed. ESR and SANS results of the bile salt micelles are compared and discussed.

2. Experimental

2.1 *Materials*

NaC and NaDC samples from Sigma Chemical Co. (USA) were used as such. Sigma D_2O was used instead of water. Quantitatively weighed amounts of the bile salts and D_2O were mixed and sonicated to prepare isotropically homogenous solutions. The spin probe CSL was also purchased from Sigma and was used without further purification. ESR samples were prepared by dissolving the spin probe in ethanol which was evaporated in a sample tube using nitrogen purging during which the bile salt solution was added quantitatively under constant stirring and in a sealed condition.

2.2 *SANS measurements*

SANS measurements were carried out on the spectrometer fitted with a one-dimensional position sensitive detector installed at the Dhruva Reactor, Trombay, Bhabha Atomic Research Centre, Mumbai. The experimental procedure adopted was according to the User's manual [25]. The liquid samples were taken in a quartz cell of path length 1 cm. A BeO filtered neutron beam of mean wavelength $l = 5{\cdot}2$ Å was used. The wavevector transfer Q range accessible from the instrument was 0·02 to 0·08 Å^{-1} where $Q = 4p\sin q/l$ and $2q$, the scattered angle. The data were collected for the fast neutron background up to $Q = 0{\cdot}3$ Å^{-1} and the transmission factor was normalised to the absolute cross-section units. Based on the conclusions of Berr [26] the micellar properties in D_2O were assumed to be unaltered from that of H_2O solutions, within the limits of experimental error.

The measured SANS distribution was analysed using the method of Hayter–Penfold for an assembly of monodisperse uniform ellipsoidal micelles. The coherent differential cross-section ($d\Sigma/d\Omega$) can be expressed as[27],

$$d\Sigma/d\Omega = N_m V_m^2 (r_m - r_s)^2 [\langle F^2(Q)\rangle + \langle F(Q)\rangle^2 \{S(Q) - 1\}], \quad (1)$$

where N_m is the number density of the micelles, r_m and r_s are the scattering length densities of micelle and solvent, V_m is the micelle volume, $F(Q)$ is the form factor defined as $(1/V_m)\int \exp(iQ\Sigma)d\Sigma$ that describes the angular distribution of scattering to the morphology of the micelle with respect to Q and Q being $4p\sin q/l$ respectively.

The structure factor $S(Q)$ represents interparticle interferences and has been calculated approximating the ellipsoid to an equivalent sphere of radius $R = (a^2b)^{1/3}$, where R is the effective radius of the micelle. The concentration of micelles [mic] mol dm^{-3} is known from N_{BS}, C_s and CMC as equal to (C_s-CMC)/N_{BS}. The number density of micelle in solution $N_m = N_{av}$[mic]/1000 (ml^{-1}).

2.3 *ESR measurements*

In ESR measurements, sample solutions were injected into the capillary tubes incubating at 25 ± 0·05°C, using a Varian E-112 EPR instrument fitted with temperature controller with the usual spectrometer settings such as 100 kHz modulation amplitude, microwave power 8 mW, scan range 100 G and scan speed 8 min.

3. Results and discussion

The measured and fitted SANS distribution for NaC and NaDC secondary micelles in 0·1 M solutions are shown in figure 1. Best-fit results are found for monodisperse ellipsoidal models of NaC and NaDC micelles. The SANS distributions developed correlation peaks around $Q = 0{\cdot}12$ and 0·1 Å^{-1} for NaC and NaDC micelles. The shifting to shorter Q values for constant concentrations of bile salt indicate increasing average intermicellar distance ($d = 2p/Q_{max}$) with $Q_{max} = Q$ at peak position, i.e. when secondary micelles are formed due to the association of primary micelles, the number density of primary micelles tends to decrease. This effect causes an increase in the average intermicellar distance. The other micellar parameters obtained from SANS data after applying Hayter–Penfold type of analysis for NaC and NaDC are presented in table 1. The ellipsoidal micelles of pure NaC and NaDC with semi-minor axes ($a = c = 8$ Å) and semi-major axis ($b = 18{\cdot}4$ Å and 31·7 Å) produce best-fit results and correspond to the

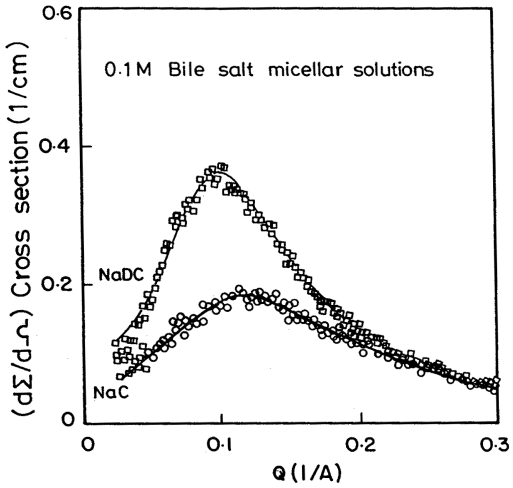

Figure 1. Small angle neutron scattering data of sodium cholate (NaC) and sodium deoxycholate (NaDC) secondary micelles in D_2O solution at 25°C.

Table 1. Micellar parameters of 0·1 M D_2O solutions of sodium cholate and sodium deoxycholate secondary micelles at 298 K.

Parameters	NaC	NaDC
R (Å)	10·6	12·7
$a = c$(Å)	8·0	8·0
b(Å)	18·4	31·7
N_{BS}	9·1	16·2
[mic] $\times 10^3$ (mol dm^{-3})	9·34	5·86
$N_m \times 10^{-18}$ (dm^{-3})	5·62	3·53
d(Å)	52·4	62·8
a	0·79	0·62
k^{-1} (Å)	4·1	3·5
$U(r)/U(T) \times 10^{-5}$ (K_BT) units	0·0115	0·0227
$t_B \times 10^9$ (s)	3·2	5·8
$t_C \times 10^9$ (s)	2·45	3·3
$t_R \times 10^9$ (s)	2·8	4·38
R_h(Å)	14·2	16·3
R*(Å)	15·0	17·0

*Value from Ref. [18] for NaDC; from Ref. [36] for NaC

dimensions of secondary micelles. The equivalent spherical radii values seem to be in agreement with those in the literature [28]. Equation (1) representing Hayter–Penfold best-fits produces N_m values of strongly interacting micelles in aqueous media. Bile salt micelles being anionic with $(1 - a)$ being the fraction of the bound counterions (Na^+) per micelle, the Debye screening length k^{-1} is given as $[8pN_{av}e^2I/1000xK_BT]^{1/2}$ where I is the ionic strength = (CMC + aC_s)/2 where C_s is the concentration of the bile salt, x is the dielectric constant of D_2O = 78·25, K_B is the Boltzmann constant and e is the electronic charge. The intermicellar interaction potential in terms of the screened coulomb

potential of ionic micelles $U(r)$ and the contact potential $U(T)$ is taken as $U(r)/U(T) = \exp[-(r - s)/kr]$, where r is the intermicellar distance that is equivalent to d since $d \gg R$ and $s = 2R$ respectively.

In figure 2, the ESR spectra of the spin probe CSL solubilised NaC and NaDC aqueous solutions are given. Since the ESR spectra recorded on blank solutions of bile salt did not give any signal and the ESR spectra of the ethanolic solution of the spin probe produced t_R values very much lower than that of the micellar solutions, the observed ESR spectrum (figure 2) distinctly represents the interaction of the spin probe with the micelles [29–31]. Using (2)–(4), the rotational correlation times t_R are calculated and listed in table 1.

$$t_R = (t_B . t_C)^{1/2}, \tag{2}$$

where $t_B = C_1 \cdot B$ and $t_C = C_2 \cdot C$, and

$$B = -\tfrac{1}{2}\Delta H_0\{(I_0/I_1)^{1/2} - (I_0/I_{-1})^{1/2}\}; C_1 = 1{\cdot}27 \times 10^{-9}, \tag{3}$$

$$C = \tfrac{1}{2}\Delta H_0\{(I_0/I_1)^{1/2} + (I_0/I_{-1})^{1/2} - 2\}; C_1 = 1{\cdot}19 \times 10^{-9}. \tag{4}$$

For the nitroxide spin probe used here, the principal g factors and hyperfine splitting factors are: $g_{xx} = 2{\cdot}009$; $g_{yy} = 2{\cdot}006$; $g_{zz} = 2{\cdot}002$, $A_{xx} = A_{yy} = 6$ G; $A_{zz} = 32$ G. ΔH_0 refers to the peak-to-peak line width of the centre line; I_0, I_1 and I_{-1} are the amplitudes of the low, centre and high field lines in the 3-line spectra of the spin probe. The hydrodynamic equivalent spherical radii of the micelles are calculated from the t_R values using the Stokes–Einstein relation for rotational diffusion motion of the micelles, i.e., $t_R = 4\pi\eta R_h^3/3K_BT$, where η is the solvent viscosity, $T = 298$ K and K_B = Boltzmann constant.

Regarding the secondary micellization process, bile salts differ from those of classical surfactants. This is because bile salt molecules have the hydrophobic surface at the convex side (b side) of the steroid nucleus and the hydrophilic surface consisting of hydroxyl and carboxylate groups at the concave side (a side) of the steroid nucleus.

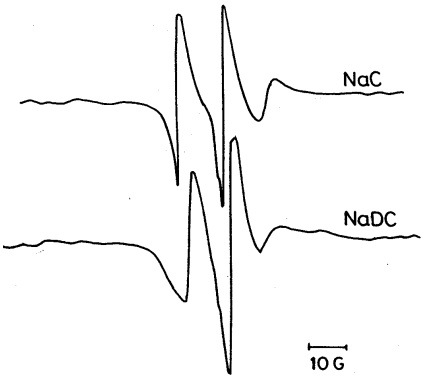

Figure 2. ESR of 0·1 M bile salts solubilised with the spin probe CSL.

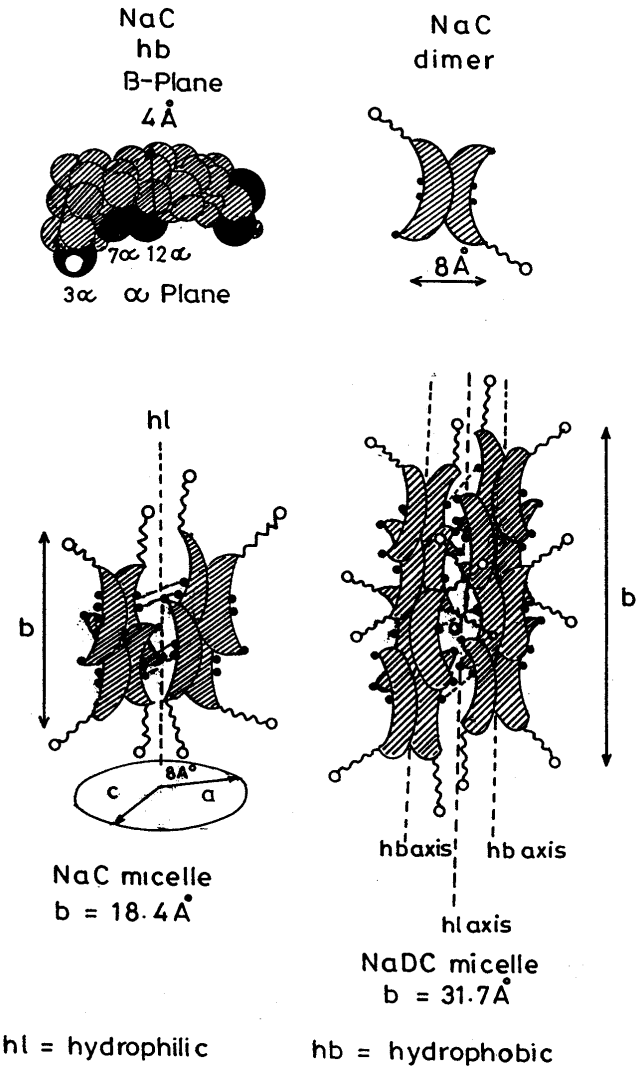

Figure 3. Structures of secondary micelles of sodium cholate (NaC) and sodium deoxycholate (NaDC).

Interaction among the hydrophobic faces results in micelle formation[32]. Secondary micelles are developed due to the aggregation of primary micelles favoured by the H-bonding forces among the hydrophilic faces. During the formation of secondary micelles, rod-like micelles constituting discrete regions of both hydrophilic (H-bonding) and hydrophobic bonding exist. In figure 3, schematic representation of the super grown NaC and NaDC micelles are depicted with different hydrophobic and hydrophilic regions. Commonly the free bile acid molecules are about 20–21 Å long, from end to end. The steroid nucleus is not flat but circular in cross-section. The width of the steroid nuclei between the *a* and *b* surfaces is nearly 3·5–4 Å units. Using the effective radius (*R*) value, volume per micelle may be determined[33]. Knowing volume per bile salt molecule in the anhydrous sodium salt condition is 539 $Å^3$ and 526 $Å^3$ respectively for NaC and

NaDC molecules, approximate N_{BS} values are deduced [34]. Since SANS estimations involve only the hard core radii values and not the hydrodynamic ones, the anhydrous volumes of bile salt molecules are considered. In doing so, N_{BS} values per super grown micelles are nearly 9·0 and 16·0 for NaC and NaDC systems. This is one reason for the higher intensity of the SANS curve for the NaDC than for the NaC micelle systems (figure 1).

Regarding the structural properties of the secondary micelles, microstructures of the NaC micelles as depicted in the scheme coincide well with those reported in the literature [35]. However bile salt secondary micelles consisting of units of tetramers (*b* in scheme) can be built up along the horizontal way (axis *a*) through H-bondings or along the vertical way (axis *b*) which is mainly favoured by hydrophobic forces. SANS data presently predict hydrophobically grown micelles of NaDC rather than the other form which is based mainly on the semi-major axis value of the ellipsoid and is nearly twice as that of the NaC when the semi-minor axes are the same. This type of the process of growth in the micelle is favoured under high concentrations of bile salts while growth is favoured mainly by the hydrophilic forces under high ionic strengths of the medium with high concentrations of the counterions [36]. Counterion condensation favours micellar growth. It is observed that a of NaDC is lower than that of NaC. This indicate clearly that screening of coulombic potentials between the micelles occurs to a greater extent in NaDC than in NaC. Screened coulombic forces favour hydrophobic binding. Hence rod-like micelles with hydrophilic bonds at the central axis of the rod, seems the best-fit picture of the secondary micelle of NaDC.

Considering R and R_h values from SANS and ESR measurements, R_h values are found to be greater. Values of R are deduced from the core radii values. The discrepancy in the value is equivalent to the Debye screening length of the ionic micelles. Thus the equivalent spherical radius value evaluated from a and b values when corrected with hydration layer thickness, gives comparable R_h values, i.e., the hydrodynamic semi-minor (a_h) and semi-major (b_h) radii values of NaC are $(a + k^{-1}) = 12{\cdot}1$ Å and $(b + k^{-1}) = 22{\cdot}5$ Å. The hydrodynamic equivalent spherical radius value calculated from a_h and b_h $[= (a_h^2 \cdot b_h)^{1/3}]$ is 14·9 Å. Similarly for the NaDC system the hydrodynamic equivalent spherical radius value is 16·7 Å.

These values are in agreement with the R_h values obtained from ESR measurements (table 1). The intermicellar interaction potential, $U(r)/U(T)$ in terms of K_BT units is calculated from the SANS data (table 1) and for NaDC micelles, the values are twice as much as those for NaC micelles. Comparing reports on the size and shape of bile salt micelles grown as single crystals, the views may be extended as below. The hydrophobic axis parallel to the hydrophilic central axis, concentric to the hydrophilic central axis of the prolate ellipsoids of bile salt micelles (NaDC), helically winds around the central axis if further growth along the major axis takes place. If concentration of bile salt is not very high, then short prolate micelles as in the present case would exist in solution wherein the helical nature of the hydrophobic axis may not be seen. In such a case, the observed data agree well with those of the literature [9].

Acknowledgement

The authors thank the Inter-University Consortium for DAE Facilities, Government of India for financial assistance and for the permission to procure SANS data from the Dhruva Reactor at BARC, Mumbai (Project No. CRS-M-62).

References

1. Esumi K and Ueno M (eds) 1997 *Structure–performance relationships in surfactants* (Surfactant Science Series) (New York: Marcel Dekker) vol 70, chap. 3, pp 147–195
2. Small D M 1971 *The bile acid* (New York: Plenum) vol 1, p. 302
3. Borgtstrom B, Barrowman J A and Lindstrom M 1985 In *Sterols and bile acid* (eds) H Danielsson and J Sjoval (Amsterdam: Elsevier)
4. Small D M, Penkett S and Chapman D 1969 *Biochim. Biophys. Acta* **176** 178
5. Bourges M, Small D M and Dervichian D G 1967 *Biochim. Biophys. Acta* **144** 189
6. Small D M 1968 *J. Am. Oil Chem. Soc*. **45** 198
7. Oakenful D G and Fisher L R 1977 *J. Phys. Chem*. **81** 1838
8. Zakrzewska J, Markovic V, Vucelic D, Feigin L, Dembo A and Mogilevsky L 1990 *J. Phys. Chem*. **94** 5079
9. Esposito G, Giglio E, Pavel N V and Zanobi A 1987 *J. Phys. Chem*. **91** 356
10. Hao L, Lu R, Least D G and Poulin P R 1997 *J. Solution Chem*. **26** 113
11. Coello A, Meijide F, Rodriguez Nunez E and Vazquez Tato J 1993 *J. Phys. Chem.* **97** 10186
12. Pedersen J S, Egelhaaf S and Schurtenberger P 1995 *J. Phys. Chem*. **99** 1299
13. Cohen D E, Thurston G M, Chamberlin R A, Benedek G B and Carey M C 1998 *Biochemistry* **37** 14798
14. Conte G, Di Blasi R, Giglio E, Parretta A and Pavel N V 1984 *J. Phys. Chem.* **88** 5720
15. O'Connor C J, Ch'ng B T and Wallace R G 1983 *J. Coll. Int. Sci*. **95** 410
16. Coello A, Meijide F, Rodriguez Nunez E and Vazquez Tato J 1996 *J. Pharm. Sci*. **85** 9
17. Hjelm R P, Schteingart C D, Hofmann A F and Thiagarajan P 2000 *J. Phys. Chem.* **B104** 197
18. Lopez F, Samseth J, Mortensen K, Rosenqvist E and Rouch J 1996 *Langmuir* **12** 6188
19. Igimi H and Carey M C 1980 *J. Lipid Res*. **21** 72
20. Goyal P S, Chakravarthy R, Dasannacharya B A, Desa J A E, Kelkar V K, Manohar C, Narasimhan S L, Rao K R and Valaulikar B S 1989 *Physica* **156** 471
21. Goyal P S, Dasannacharya B A, Kelkar V K, Manohar C, Srinivasa Rao K and Valaulikar B S 1991 *Physica* **174** 196
22. Kawamura H, Murata Y, Yamaguchi T, Igimi H, Tanaka M, Sugihara G and Kratohvil J P 1989 *J. Phys. Chem*. **93** 3321
23. Kratohvil J P 1984 *Hepatology* **4** 85S
24. Cannon B, Polnaszek C F, Butler K W, Erikson K E G and Smith I C P 1975 *Arch. Biochim. Biophys*. **167** 505
25. Goyal P S, Aswal V K and Joshi V 1995 In *User's manual for position sensitive detector based small angle neutron scattering spectrometer*, Bhabha Atomic Research Centre, Mumbai, Government of India
26. Berr S S 1987 *J. Phys. Chem.* **91** 4760
27. Santhanalakshmi J, Goyal P S, Aswal V K and Vijayalakshmi G 1999 *Proc. Indian Acad. Sci*. (*Chem. Sci*.) **111** 651
28. Young C Y, Missel P J, Mazer N A, Benedek G B and Carey M C 1978 *J. Phys. Chem.* **82** 1375
29. Schreier S, Polnaszek C F and Smith I C P 1978 *Biochim. Biophys. Acta* **515** 375
30. Polnaszek C F 1976 In *Spin labelling theory and applications* (ed.) L J Berliner (New York: Academic Press)
31. Kooser R G, Volland W V and Freed J H 1969 *J. Chem. Phys.* **50** 5243
32. Blow D M and Rich A 1959 *Nature (London)* **182** 3566
33. Esposito G and Giglio E 1987 *J. Phys. Chem.* **91** 356
34. Small D M 1968 *Adv. Chem. Ser.* **84** 31
35. Dembo A T, Sosfenov N I and Feigin L A 1966 *Sov. Phys. Crystallogr. (Engl. Transl.)* **581** 19
36. Mazer N A, Carey M C, Kwasnick R F and Benedek G B 1979 *Biochemistry* **18** 3064